NUCLEAR SCIENCE AND TECHNIQUES **26**, 060402 (2015)

A novel compact Tokamak Hard X-ray diagnostic detector*

CAO Jing (曹靖),[1,2] JIANG Chun-Yu (蒋春雨),[1,2] ZHAO Yan-Feng (赵艳凤),[1,2]
YANG Qing-Wei (杨青巍),[3] and YIN Ze-Jie (阴泽杰)[1,2,†]

[1] *State Key Laboratory of Particle Detection and Electronics, University of Science and Technology of China, Hefei 230026, China*
[2] *Department of Modern Physics, University of Science and Technology of China, Hefei 230026, China*
[3] *Southwestern Institute of Physics, Chengdu 610041, China*

(Received October 21, 2014; accepted in revised form December 19, 2014; published online December 20, 2015)

A compact X-ray detector based on the lutetium yttrium oxyorthosilicate scintillator (LYSO) and silicon photomultiplier (SiPM) has been designed and fabricated for the hard X-ray diagnosis on the HL_2A and HL_2M Tokamak devices. The LYSO scintillator and SiPM in small dimensions were combined in a heat shrink tube package, making the detector compact and integrative. The Monte Carlo particle transport simulation tool, Geant4, was utilized for the design of the detector for the hard X-ray from 10 keV to 200 keV and the best structure scheme was presented. Finally, the detector was used to measure the photon spectrum of a ^{137}Cs gamma source with a pre-amplifier and a multichannel amplitude analyzer. The measured spectrum is consistent with the theoretic spectrum, it has shown that the energy resolution of the detector is less than 14.8% at an energy of 662 keV.

Keywords: Hard X-ray, Tokamak, HL_2A/HL_2M, Lutetium yttrium oxyorthosilicate scintillator (LYSO), Silicon photomultiplier (SiPM), Geant4

DOI: 10.13538/j.1001-8042/nst.26.060402

I. INTRODUCTION

Hard X-ray diagnosis is one of the main diagnoses for Tokamak devices. Under Lower Hybrid Current Drive (LHCD), measuring the emitted hard X-ray from the plasma area is an important diagnostic method to study the current drive efficiency, electron speed spatial distribution, energy deposition, and other physical conditions [1]. LHCD is a commonly used non-inductive heating method in Tokamak experiments. It will heat the hot electrons to a resonance energy about 10 keV to 200 keV, thus the emitted bremsstrahlung hard X-ray energy range is from 10 keV to 200 keV [2]. The selection of a suitable detector is the key to this hard X-ray measurement.

A NaI scintillator was used by Goeler for the Princeton Large Torus (PLT) device in 1985 [3]; Yang *et al*. established a HgI_2 semiconductor detector to study the 15–150 keV hard X-ray for HL_1M in 1997 [1]; Peysson *et al*. introduced a CdTe detector array on the Tore Supra device and provided nice experimental diagnostic results in 2001 [4, 5]; also, CdTe detector arrays were established on the HL-7 [6], HL_2A [7–9] Tokamak. In this work, a LYSO scintillator [10–12] was chosen for its better temporal resolution compared with currently used semiconductor detector such as CdTe or CdZnTe [13, 14], the decay time of the LYSO crystal shining was only about 41 ns [15]. This means the LYSO detector can support a higher pulse count rate and has a wider dynamic range for hard X-ray measurements. The high price of CdTe and CdZnTe detectors also limits its application. Moreover semiconductor detectors are facing the problem of irradiation damage, incomplete carrier collection, and large dark current, though its energy resolution is better.

The LYSO scintillator has a high light output (76% of NaI(Tl)), large effective atomic number (65), and great density (7.1 g/cm^3), thus it has a good X-ray stopping ability and detection efficiency. It also has stable physical and chemical properties. For example, its temperature is quite small (-0.2% /°C) and it has superb radiation hardness [16]. In this work, SiPM [17, 18] was selected as the photoelectric converter due to its insensitivity to the magnetic field, suitable to work in the complex electromagnetic field around Tokamak devices. SiPM was made up of an avalanche diode array working in Geiger mode, it's quite sensitive with single photon detection capacity and has a high gain (up to 10^6), a low bias voltage, and a compact structure. This paper will describe the design, fabrication and performance of a compact Tokamak hard X-ray diagnostic detector. Its simulation and experimental results will also be presented.

II. SIMULATION

Monte Carlo particle transport simulation tools, such as Geant4 [19, 20], MCNP, and FLUKA, were widely used in the design of particle detectors, avoiding the time and costs consuming associated with detector hardware changes. Usually, we search for the perfect design by Monte Carlo simulation and predict the property and efficiency of the designed detectors. Geant4 is quite popular among these applications.

In this work, Geant4.10.00.p02 version was used. LYSO was designed to be covered with thin aluminium foil, except for the back surface. SiPM was next to the LYSO on the backside. The aluminium foil not only filters low energy X-rays under 10 keV, but also prevents the outside visible photons

* Supported by the National Natural Science Foundation of China (Nos. 11375263 and 11375195) and National magnetic confinement fusion Science Program of China (No. 2013GB104003)
† Corresponding author, zjyin@ustc.edu.cn

from entering LYSO and reflects the inside scintillate photons to be gathered by the backside SiPM. In the simulation environment, shown in Fig. 1, an X-ray source irradiates the front side of the detector comprised of an LYSO, SiPM, and aluminium foil cover. The incident X-ray is set to be a beam with radius of 1mm (on real measurement the Tokamak Hard X-ray would be collimated to enter the detector due to the requirements of spacial resolution).

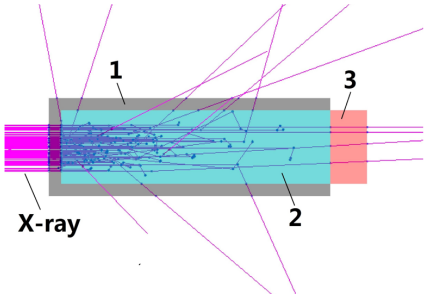

Fig. 1. (Color online) The Geant4 simulation environment of this detector under X-ray irradiation. Part 1 is the aluminium foil cover, its material is Al with density of 2.7 g/cm^3; Part 2 is the LYSO scintillation crystal, its material is $Lu_{0.6}Y_{1.397}Ce_{0.003}(SiO_4)O$ based on the LYSO products purchased from Shanghai Institute of Ceramics with density of 7.1 g/cm^3; Part 3 is the SiPM.

Firstly, the suitable aluminium foil thickness was figured out through simulation. The aluminium foil cover should filter the low energy X-ray under 10 keV and absorb a few X-rays on the focused 10–200 keV energy range, thus the performance of different thicknesses of aluminium foil (Part 1 in Fig. 1) was studied. In the simulation, the thickness is set to be 0.01, 0.05, 0.1 and 0.2 mm, respectively, 5 million X-ray photons were simulated for each energy point. The energy deposition in the front aluminium foil was compared to the incident X-ray intensity. Finally, the stopping efficiency of the aluminium foil for X-rays is calculated and shown in Fig. 2. It can be seen that 0.05 mm is the perfect thickness. The 0.01 mm aluminium foil could not stop X-rays from 5 keV to 10 keV thoroughly and 0.1 mm, and 0.2 mm aluminium foil absorb too many X-rays from 10 keV to 30 keV, which is under the measurement of the LYSO scintillator. Therefore, the chosen aluminium foil thickness is 0.05 mm.

Secondly, a suitable size for the LYSO scintillator was studied through simulation. The length of the LYSO (Part 2 in Fig. 1) changes continuously and for each LYSO length, 10 million photons with random energy from 10 keV to 200 keV were simulated to irradiate the detector. Since the quantity of produced scintillate photons was almost proportional to the energy deposition in the LYSO (about 8 000 photons per MeV), we just need to gather the energy deposition in the LYSO during the simulation, avoiding the time-consuming and inefficient large track of optical photons. After gathering the energy deposition in LYSOs of different lengths, the detection efficiency curve was calculated in Fig. 3 (Detection efficiency is the proportion of the energy deposition in total energy of the incident X-ray.). Based on Fig. 3, the ideal length of the LYSO is determined to be 11 mm, because LYSO's absorption of 10–200 keV X-ray is saturated at this length. Accordingly, longer LYSOs could not bring significant improvement in detection efficiency.

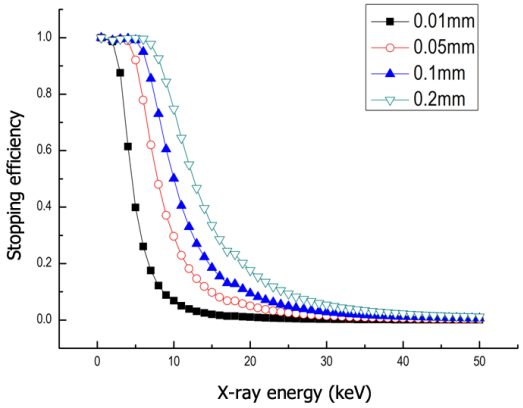

Fig. 2. (Color online) The aluminium foil stopping efficiency for X-ray from 1 keV to 50 keV.

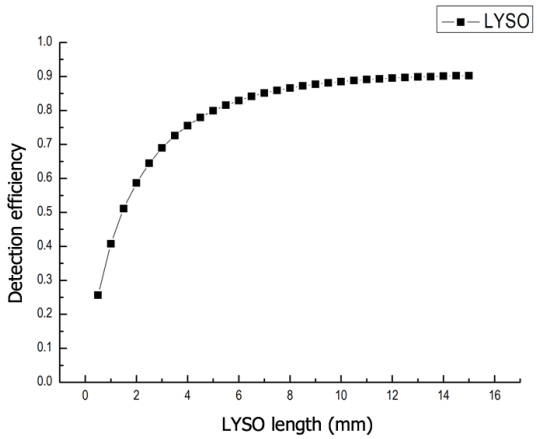

Fig. 3. The curve of LYSO detection efficiency which varies with the length of the LYSO.

For the scintillation crystal, if the incident X-ray energy is higher than the energy of its elements' characteristic X-rays, these elements will be excited and emit their characteristic X-ray. The characteristic X-rays are isotropous, therefore they have a large possibility to escape from the detector's side, causing a decrease in detection efficiency. One possible solution is to increase the size of the detector. In order to validate the effectiveness of this method, a simulation is started. The incident X-rays are fixed to irradiate the central circular region (Fig. 1) with a radius of 1 mm, the side length of the cuboid LYSO scintillator is set to be 2 mm, 3 mm and 4 mm, respectively. The mono-energy incident X-rays are changed from 1 keV to 200 keV with 1 keV the energy interval and 1 million photons simulated for each energy point. The curve of detection efficiency versus X-ray energy for the three different size LYSOs is illustrated in Fig. 4. Two sudden changes in the curves can be seen in Fig. 4. One refers to the energy point at 18 keV, as it exceeds of the

17.037 keV characteristic X-ray energy of the element Yttrium in the LYSO, Yttrium is excited. The other refers to the energy point at 64 keV, since the characteristic X-ray energy of the element Lutetium in the LYSO is 63.304 keV, Lutetium is excited. It can also been seen that after the excitation of the characteristic X-rays of Lutetium ($>$ 63 keV energy region), thicker a LYSO has a better performance of detection efficiency. Significant improvement can be observed in the 3 mm-side-length LYSO, compared to the 2 mm one, but the 4 mm-side-length LYSO only brings a slight increase in detection efficiency, compared to the 3 mm one, under the consideration of efficiency and spacial resolution, the best side length for the LYSO is 3 mm.

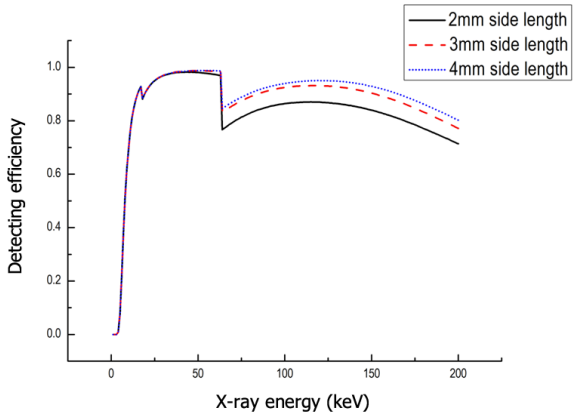

Fig. 4. (Color online) The detection efficency of LYSO with three different sizes in energy region of 1–200 keV.

III. DETECTOR AND MEASUREMENT

Based on the simulation, a suitable size for the LYSO is 3 mm $\times$ 3 mm $\times$ 11 mm for a cuboid structure. These custom-made LYSO scintillation crystals were manufactured by Shanghai Institute of Ceramics. SiPM chips were purchased from SensL Ltd. of Ireland, which are the latest B-series (type: MircroFB-30035-SMT), whose sensitive area is 3 mm $\times$ 3 mm, adapted to the LYSO size. It has 4774 microcells of avalanche diode with a size of 35 µm on the sensitive area; the operating voltage is from 25.5 V to 29.5 V (breakdown voltage is 24.5 V, overvoltage range is from 1 V to 5 V); its peak wavelength of absorbed optical photons is 420 nm, also adapted to the average 420 nm scintillate photon wavelength of the LYSO. It has two signal outputs, one is an anode to cathode readout with a gain of 3×10^6 and the other is a fast terminal readout with a gain of 4.3×10^4, which is the selected readout in this work. The output signal by fast terminal readout has a rise time of 0.6 ns and a pulse width of 1.5 ns, an order of magnitude less than the 41 ns decay time of the LYSO crystal shining, making the final output signal pulse width mainly determined by crystal shining decay time. The aluminium foil thickness is 0.05 mm, as required. The LYSO, SiPM and aluminium foil are shown in Fig. 5.

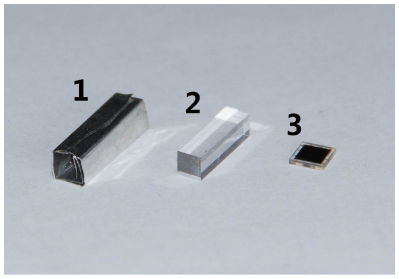

Fig. 5. The selected LYSO scintillation crystal, SiPM and the aluminium foil. Part 1 is the aluminium foil with a thickness of 0.05 mm; Part 2 is the 3 mm $\times$ 3 mm $\times$ 11 mm LYSO; Part 3 is the SiPM chip in the SMT package.

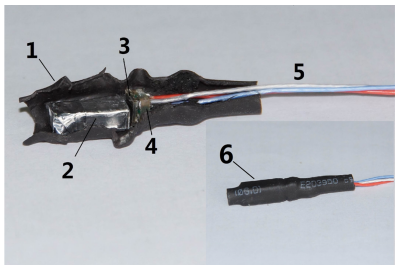

Fig. 6. The real photo of the compact detector and its inside structure. Part 1 is the heat shrink tube package when split to show the inner structure; Part 2 is the aluminium foil covered LYSO scintillator; Part 3 is the SiPM chip; Part 4 is the small bonding pad for the SMT packaged SiPM chip; Part 5 is the signal and power wires; Part 6 is the outside appearance of the detector.

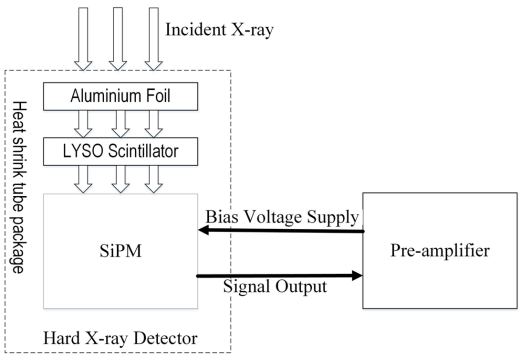

Fig. 7. The block diagram of the compact Hard X-ray detector.

The detector was finally fabricated and then packaged in a heat shrink tube, as shown in Fig. 6, its block diagram is also presented in Fig. 7. The sensitive area of SiPM was close to the uncovered backside surface of the LYSO, the other side of the LYSO is covered with 0.05 mm of aluminium foil. The heat shrink tube not only fix all the parts together, but also stop outside visible photons from entering the SiPM from the small gap between LYSO and SiPM sensitive areas. Three power and signal wires were collected to the small bonding pad where SiPM is welded on. Since, in future use, the detectors will be right next to the pre-amplifier or even fixed on the PCB board of the pre-amplifier, EM interferences of the short

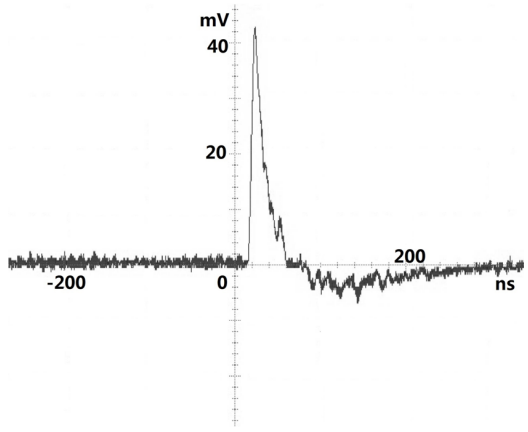

Fig. 8. The fast terminal readout signal pulse of the detector.

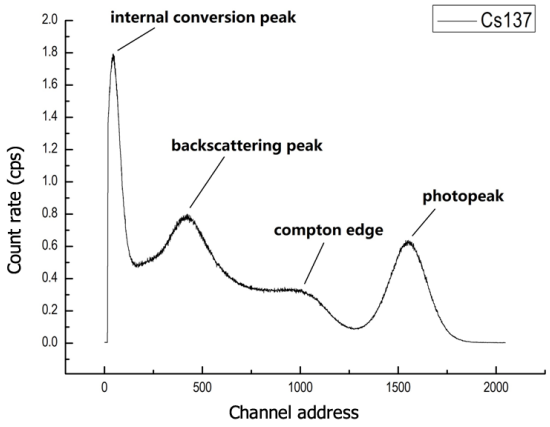

Fig. 9. The measured pulse amplitude spectrum for the ^{137}Cs gamma source.

signal wires could be ignored, as coaxial cable is not used in its signal transmission.

The detector was used to measure a ^{137}Cs gamma source, whose typical fast terminal readout signal is shown in Fig. 8. It can be seen that the signal has some undershoots, because the fast terminal output pulse signals are alternating current coupled. The signal has a width of about 50 ns and an amplitude of 42 mV, corresponding well to the 41 ns LYSO shinning decay time and 1.5 ns SiPM signal width.

A pre-amplifier was used to amplify the signals from the detectors, and the amplified signals were analyzed by a multichannel amplitude analyzer. The 2048-channel pulse amplitude spectrum was measured for the ^{137}Cs gamma source as shown in Fig. 9. The measured spectrum is consistent with the theoretic ^{137}Cs gamma spectrum. The spectrum structures, such as the photopeak, Compton edge, backscattering peak and internal conversion peak, were present. From the photopeak, we calculated the energy resolution of this detector at an energy of 662 keV, which is 14.8% of the effects of the pre-amplifier and multichannel amplitude analyzer.

IV. CONCLUSION

In this work, a Tokamak Hard X-ray diagnostic detector based on the LYSO and SiPM was designed and fabricated. Compared to semiconductor detectors, such as CdTe and CdZnTe, though having a worse energy resolution, its fast signal output has made it capable of reaching a higher pulse count rate. Thus, it will adapt to hard X-ray with greater intensity and has a wider dynamic range, making it another potential hard X-ray diagnosis detector. Also, its cost advantage over other semiconductor detectors makes it capable of establishing a diagnostic array with more detectors to provide better spacial resolution.

The detector described in this paper is quite compact and integrative, the Geant4 simulation has validated its value in Hard X-ray diagnostics. The experiment on a ^{137}Cs gamma source has preliminarily validate its capability in photon detection, but more research needs to be done before its maturity. Since the HL-2A and HL-2M Tokamak Hard X-rays mainly concentrate on the energy region from 10 keV to 200 keV, in future works we'll continue to test the detector in this energy region, and acquire the related energy resolution. The measurement environment around the Tokamak device is complex, including the presence of neutron radiation. Accordingly, the radiation damage on SiPM and LYSO also needs to be studied. The effects of temperature change and instability of bias voltage supply on the gain of SiPM require some adjustment work. We hope in later works that the detector will be improved and real diagnostic experiments on the Tokamak using this detector will be carried out.

[1] Yang J W, Zhang G Y, Zeng C X, *et al*. Measurement and Study of Hard X-ray Bremsstrahlung emission with LHCD in the HL-1M Tokamak. Nucl Fusion Plasma Phys, 1997, **17**: 28–33. (in Chinese)
[2] Li J R, Lin S Y, Zhu W, *et al*. Study on EAST horizontal hard X-ray diagnostic unit. Vacuum, 2009, **46**: 79–82. (in Chinese) DOI: 10.13385/j.cnki.vacuum.2009.04.026
[3] Goeler S V, Stevens J, Bernabei S, *et al*. Angular Distribution of the Bremsstrahlung emission during lower hybrid current drive on PLT. Nucl Fusion, 1985, **25**: 1515–1528. DOI: 10.1088/0029-5515/25/11/001
[4] Peysson Y and Arslanbekov R. Measurement of the non-thermal bremsstrahlung emission between 30 and 200 keV with a high time-space resolution on the tokamak TORE SUPRA. Nucl Instrum Meth A, 1996, **380**: 423–426. DOI: 10.1016/S0168-9002(96)00316-6
[5] Peysson Y, Coda S and Imbeaux F. Hard X-ray CdTe tomography of tokamak fusion plasmas. Nucl Instrum Methods A, 2001, **458**: 269–274. DOI: 10.1016/S0168-9002(00)00870-6
[6] Lin S Y, Shi Y J, Wan B N, *et al*. Hard X-ray PHA system on the HT-7 tokamak. Plasma Sci Technol, 2006, **8**: 261–264.
[7] Zhang Y P, Mazon D, Liu Y, *et al*. Hard X-ray camera sys-

tem planned for HL-2A tokamak fast electron bremsstrahlung tomography. Fusion Sci Technol, 2014, **65**: 366–371. DOI: 10.13182/FST13-695

[8] Zhang Y P, Liu Y, Song X Y, *et al*. Measurements of the fast electron bremsstrahlung emission during electron cyclotron resonance heating in the HL-2A tokamak. Rev Sci Instrum, 2010, **81**: 103501. DOI: 10.1063/1.3488966

[9] Duan X R, Ding X T, Dong J Q, *et al*. Overview of experimental results on HL-2A. Nucl Fusion, 2009, **49**: 104012. DOI: 10.1088/0029-5515/49/10/104012

[10] Melcher C L and Schweitzer J S. Cerium-doped lutetium oxyorthosilicate: A fast, efficient new scintillator. IEEE T Nucl Sci, 1992, **39**: 502–505. DOI: 10.1109/23.159655

[11] Lecomte R, Pepin C, Rouleau D, *et al*. Investigation of GSO, LSO and YSO scintillators using reverse avalanche photodiodes. IEEE T Nucl Sci, 1998, **45**: 478–482. DOI: 10.1109/23.682430

[12] Pepin C M, Bérard P, Perrot A L, *et al*. Properties of LYSO and recent LSO scintillators for phoswich PET detectors. IEEE T Nucl Sci, 2004, **51**: 789–795. DOI: 10.1109/TNS.2004.829781

[13] Takahashi T and Watanabe S. Recent progress in CdTe and CdZnTe detectors. IEEE T Nucl Sci, 2001, **48**: 950–959. DOI: 10.1109/23.958705

[14] Niu L B, Li Y L, Zhang L, *et al*. Performance simulation and structure design of Binode CdZnTe gamma-ray detector. Nucl Sci Tech, 2014, **25**: 010406. DOI: 10.13538/j.1001-8042/nst.25.010406

[15] Nassalski A, Kapusta M, Batsch T, *et al*. Comparative study of scintillators for PET/CT detectors. IEEE T Nucl Sci, 2007, **54**: 3–10. DOI: 10.1109/TNS.2006.890013

[16] Zhang L Y, Mao R H, Yang F, *et al*. LSO/LYSO crystals for calorimeters in future HEP experiments. IEEE T Nucl Sci, 2014, **61**: 483–488. DOI: 10.1109/TNS.2013.2279993

[17] Buzhan P, Dolgoshein B, Filatov L, *et al*. Silicon photomultiplier and its possible applications. Nucl Instrum Methods A, 2003, **504**: 48–52. DOI: 10.1016/S0168-9002(03)00749-6

[18] Dolinsky S, Fu G and Ivan A. Timing resolution performance comparison of different SiPM devices. Nucl Instrum Methods A, 2015, **801**: 11–20. DOI: 10.1016/j.nima.2015.08.024

[19] Agostinelli S, Allison J, Amako K, *et al*. Geant4–a simulation toolkit. Nucl Instrum Meth A, 2003, **506**: 250–303. DOI: 10.1016/S0168-9002(03)01368-8

[20] Tang S B, Yin Z J, Huang H, *et al*. Geant4 used in medical physics and hadrontherapy technique. Nucl Sci Tech, 2006, **17**: 276–279.